Chinese Chemical Letters 34 (2023) 108592

Contents lists available at ScienceDirect

Chinese Chemical Letters

journal homepage: www.elsevier.com/locate/cclet

Chemo–immunotherapy for chemo-resistance and metastasis of triple-negative breast cancer by combination of iron-oxide nanoparticles and dual-targeting doxorubicin liposomes

Heping Hu[a], Lijia Yu[b], Zhao Ding[c], Jinsong Ding[d], Yiguo Hu[e], Zongning Yin[a,*]

[a] Key Laboratory of Drug Targeting and Drug Delivery System of Ministry of Education, West China School of Pharmacy, Sichuan University, Chengdu 610041, China
[b] Sichuan Huiyu Seacross Medical Technology Co., Ltd., Chengdu 610031, China
[c] Sichuan Huiyu Pharmaceutical Co., Ltd., Neijiang 641000, China
[d] Xiangya School of Pharmaceutical Sciences, Central South University, Changsha 410013, China
[e] State Key Laboratory of Biotherapy and Cancer Center, West China Hospital, Sichuan University, and Collaborative Innovation Center for Biotherapy, Chengdu 610044, China

ARTICLE INFO

Article history:
Received 5 February 2023
Revised 13 May 2023
Accepted 18 May 2023
Available online 19 May 2023

Keywords:
Multidrug resistance
Multiorgan-specific metastases
Immunogenic cell death
Intermittent dosing
Immunosuppressive tumor microenvironment
Tumor-associated macrophages

ABSTRACT

Triple-negative breast cancer (TNBC) lacks specific regimens for targeted therapy. Repeat chemotherapy promotes the evolution of TNBC into highly chemo-resistant tumors that metastasize to multiple organs simultaneously. Herein, polyacrylic acid-coated ultrasmall superparamagnetic iron-oxide nanoparticles (PAA@IONs) and dual-targeting doxorubicin liposomes achieved chemo–immunotherapy through intermittent administration. They inhibited tumor-drug resistance and multiorgan-specific metastasis significantly by targeting tumors and the microenvironment. We deciphered an immunosuppressive pre-metastatic *niche* and discovered that PAA@IONs could target tumors, tumor-draining lymph nodes (TDLNs), the liver, bone, and lungs. They promoted the polarization of macrophages into M1 macrophages in these organs and tissues. This action remodeled the immunosuppressive microenvironment and induced a sustained immune response, thereby reducing organ-specific metastasis. Overcoming the disadvantages of doxorubicin-induced cardiotoxicity as well as low tumor specificity, dual peptide-modified liposomes could target CD206 and CD13 simultaneously, and reverse chemo-resistance. These properties resulted in a significant decrease in the numbers of myeloid-derived suppressor cells (MDSCs) and cancer stem cells (CSCs) in the liver, lungs, and bone, thereby reducing protein expression of Ki-67 in TDLNs, and dramatically increasing the number of cluster of differentiation (CD)8^+ T cells and $CD8^+$ T cell/T-regulatory-cell ratio in tumors and TDLNs ($P < 0.0001$). Compared with the control ($P < 0.05$ and $P < 0.01$, respectively) or free drug ($P < 0.0001$ and $P < 0.01$, respectively), multi-organ metastases were suppressed significantly, tumor-growth rate reduced, and survival prolonged. Our drug-delivery system overcame TNBC chemo-resistance and inhibited multiorgan-specific metastases. It circumvents the lack of effective therapeutic targets, the problem of patient selection due to a low mutation rate, and can simultaneously offer the possibility of avoiding surgery and considerable postoperative complications.

Triple-negative breast cancer (TNBC) is an aggressive, metastatic, and remarkably drug-resistant subtype of breast cancer without expression of the estrogen receptor, progesterone receptor, or overexpression of human epidermal growth factor receptor 2 (HER2). TNBC is not sensitive to endocrine therapy or traditional anti-HER2-targeted therapy [1]. Targeted therapies with antibody–drug conjugates, inhibitors of the phosphatidylinositol 3-kinase/protein kinase B/mammalian target of rapamycin (PI3K/Akt/mTOR) pathway, and cyclin-dependent kinase inhibitors have opened new perspectives for TNBC treatment. However, the low rate of gene mutations in TNBC and the low rate of applicability to targeted therapies remain considerable challenges in clinical practice.

Due to the low immunogenicity and immunosuppressive tumor microenvironment (TME) of TNBC, the objective response rate of TNBC patients treated with immunotherapy is only 12%–19% [2]. Therefore, neoadjuvant treatment for early TNBC and adjuvant chemotherapy for postoperative TNBC are centered mainly on

* Corresponding author.
E-mail address: yzn@scu.edu.cn (Z. Yin).

https://doi.org/10.1016/j.cclet.2023.108592
1001-8417/

anthracycline- and taxane-related compounds [3]. However, repeat chemotherapy is highly prone to the induction of resistance, and tumors metastasize to multiple organs simultaneously, which contributes to treatment failure in >90% of patients with TNBC [4].

For decades, efficacious treatment for recurrent or metastatic TNBC has been lacking. Therefore, developing a strategy of targeted treatment that can improve the sensitivity of chemotherapy and the range of patient selection is urgent. Such a strategy would inhibit metastasis by TNBC to multiple organs and improve the outcome of TNBC treatment.

The most common organs for TNBC metastasis are the lymph nodes, followed by bone, liver, lungs, and brain [5]. If a lymph node has developed metastasis, then lymph-node dissection or local radiotherapy is indicated. However, both options will cause the loss of the lymph node, trigger major complications, and affect immunity [6]. Until now, drug regimens related to lymph-node metastasis of TNBC have been reported rarely. If metastasis to solitary bone occurs, the current standard of care is bisphosphonate therapy in combination with denosumab to reduce skeletal-related events, but this treatment does not prolong survival [7]. Resection is the standard treatment for liver metastases secondary to breast cancer. However, the number of patients with liver metastases secondary to breast cancer eligible for surgery is limited because of the extent and location of disease and physical status [8]. Collectively, surgery is the standard treatment for organ-specific metastasis of TNBC. However, TNBC is extremely aggressive and progresses rapidly. A lack of non-invasive and highly sensitive methods to detect metastatic tumors, as well as the inability to completely remove these small, non-localized metastatic tumors distributed in various lymph nodes and organs by surgery, hamper the chance of cure, and also leads to substantial serious complications [9,10].

One of the key drivers of metastasis and chemo-resistance has been reported to be transforming growth factor (TGF)-β [11]. TGF-β can be secreted by tumor-associated macrophages (TAMs) in the TME. Several studies have investigated the involvement of TAMs in multidrug resistance (MDR) in breast cancer. TAMs promote MDR in breast cancer by modulating interleukin (IL)-10/IL-10 receptor/signal transducer and activator of transcription (STAT)/B-cell lymphoma 2 (Bcl-2) signaling [12]. In addition, the high levels of IL-10 secreted by TAMs are responsible for MDR in breast-cancer cells. Furthermore, the immunosuppressive function of TAMs is mediated by the secretion of TGF-β [13], as well as IL-10 [14]. These cytokines play an important part in the suppression of effector cluster of differentiation (CD)8^+ T-cell functions by direct transcriptional repression of genes encoding functional mediators, such as perforins, granzymes and cytotoxins [15]. In addition, these cytokines have been shown to suppress dendritic cell (DC) function indirectly by stimulating the amplification of regulatory T cells (Tregs) or by inhibiting different aspects of DC biology, such as DC maturation, their ability to secret IL-12, as well as their ability for antigen presentation and priming of T cells [16]. Consequently, targeting TAMs has emerged as a strategy for combating MDR and metastases in TNBC. TAMs in the TME are novel targets for the treatment of MDR and metastasis in TNBC, which may circumvent the conundrum of the lack of effective therapeutic targets in TNBC immunotherapy. Studies have shown that iron-oxide nanoparticles can target macrophages specifically, excrete slowly and be retain *in vivo* for up to weeks (or even months), thereby inhibiting tumor growth by inducing polarization of pro-inflammatory macrophages [17]. Consequently, targeting TAMs by iron-oxide nanoparticles has emerged as a strategy for remodeling the TME.

To resolve the problems mentioned above, we designed polyacrylic acid-coated ultrasmall superparamagnetic iron oxide (PAA@IONs) and dual peptide-modified co-loaded doxorubicin (Dox) and β-lapachone (Lap) liposomes (NRDL-Lip) to target tumor cells and TAMs simultaneously. This strategy was based on the influence of the TME on drug resistance, metastasis, and therapy.

Our results showed that the drug resistance of MCF-7/ADR cells could be reversed significantly *in vitro*, and that multiorgan-specific metastases could be suppressed simultaneously by intermittent chemo–immunotherapy (Fig. 1). It has been reported that macrophages can account for ≤50% of the mass in solid tumors [18]. Protumoral M2-TAMs overexpress the mannose receptor (CD206), whereas antitumoral M1-TAMs lose CD206 overexpression [19]. Based on the high expression of CD13 in tumor blood vessels and CD206 on the surface of breast-cancer (4T1 and MDA-MB-231) cells and M2-TAMs, a cyclic peptide motif cNGR-THP (sequence: CNGRCGC, Cys^1-Cys^5 disulfide) and an 11 amino-acid amphiphilic synthetic polypeptide RP-11 (sequence: KFRKAFKRFFC) were designed to co-modify liposomes targeting to tumor blood vessels and cancer cells. In this way, we could achieve simultaneous accumulation and release of Dox and Lap at the tumor site. This phenomenon could reverse drug resistance, induce robust immunogenic cell death (ICD), and remodel the local immunosuppressive TME. Studies have shown that the content of PAA@IONs is much higher in tumors, lymph nodes, liver, bone and lungs than in other tissues. Therefore, PAA@IONs could promote the polarization of macrophages into antitumoral M1-TAMs in tumor and TME. This action would reverse the TME, evoke robust immune responses continuously and, thus, inhibit organ-specific metastases in multiple organs during TNBC progression. This strategy provides a novel option for the chemo–immunotherapy of TNBC.

To construct dual-targeting liposomes, we created cNGR-THP and RP-11 by solid-phase peptide synthesis. For their preparation and characterization, see Figs. S1–S6 in Supporting information. Furthermore, these peptides were allowed to react with DSPE-PEG2000-MAL to prepare targeting phospholipid molecules by a

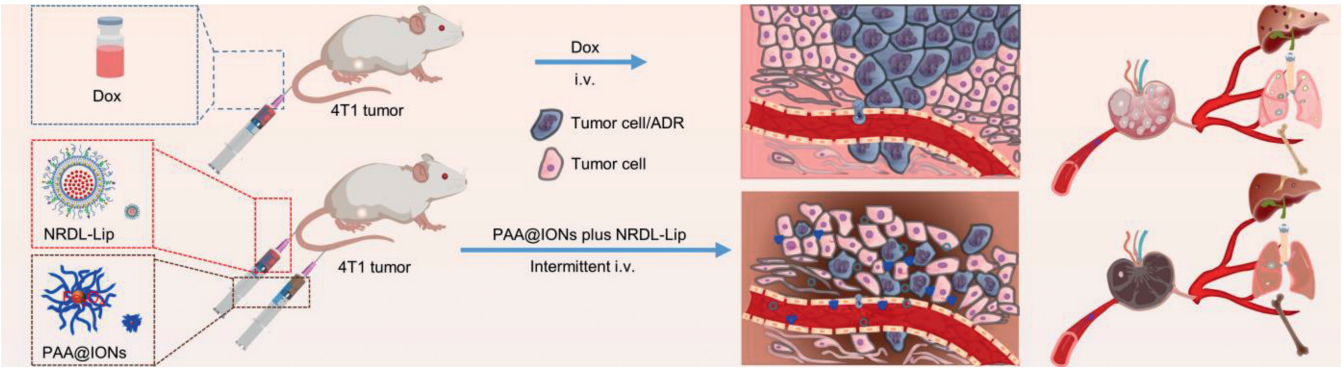

Fig. 1. PAA@IONs and NRDL-Lip targeting tumors and the microenvironment simultaneously (Schematic). This strategy can achieve chemo–immunotherapy for TNBC chemo-resistance and multiorgan-specific metastases by remodeling the immunosuppressive microenvironment.

maleimide-thiol crosslinking reaction. The liposome modified by cNGR-THP and RP-11 dual-peptide phospholipid molecules and co-loaded with Dox and Lap was called "NRDL-Lip" and was prepared by a classical thin-film hydration method (Fig. S7a in Supporting information). The mean particle size was 94.84 ± 0.16 nm, and the zeta potential was −32.4 ± 0.6 mV (Figs. S7c and d, Table S1 in Supporting information). Cryogenic transmission electron microscopy (cryo-TEM) revealed that it had a lipid-bilayer structure (Fig. S7e in Supporting information). We used similar methods to prepare the unmodified Dox liposome (Dox-Lip), the liposome co-loaded with Dox and Lap (DL-Lip), the co-loaded liposome modified with cNGR-THP (NDL-Lip), and the liposome co-loaded with RP-11 (RDL-Lip), respectively, for subsequent experiments to validate the targeting efficiency, anti-tumor and anti-resistant effects of NRDL-Lip. Microwave synthesis was used to prepare PAA@IONs (Fig. S7b in Supporting information). The nanoparticles exhibited the characteristics of ultrasmall superparamagnetic. For the details of their related physicochemical properties, see Table S1.

We undertook a cellular-uptake experiment to demonstrate that NRDL-Lip could target tumor cells and M2-TAMs. Significantly increased cellular uptake of NRDL-Lip after co-culture with MDA-MB-231 cells and M2-TAMs was observed (Figs. 2a and b). However, after adding mannose, cellular uptake reduced significantly, indicating that the mannose receptor (CD206) mediates cellular uptake of NRDL-Lip; however, cellular uptake by M1 macrophages did not decrease significantly. These results suggested

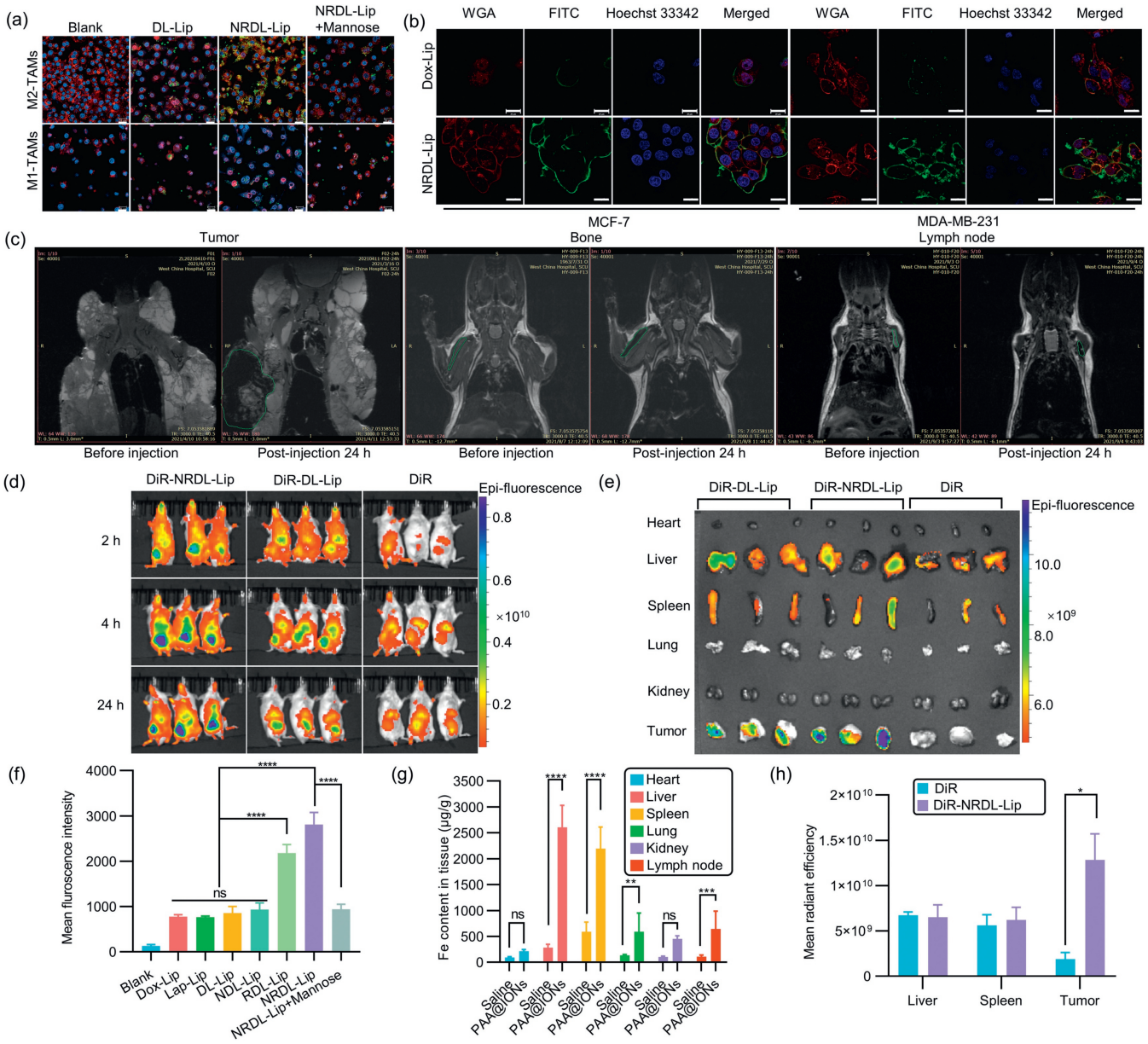

Fig. 2. *In vitro* and *in vivo* evaluation of the efficacy of NRDL-Lip and PAA@IONs dual-targeting. (a) Confocal laser scanning microscopy showing uptake in M2-TAMs and M1-TAMs treated with phosphate-buffered saline (PBS) (blank), FITC-DL-Lip, FITC-NRDL-Lip, and FITC-NRDL-Lip + mannose. 4′,6-Diamidino-2-phenylindole (DAPI) showing blue fluorescence, and wheat germ agglutinin (WGA) showing red fluorescence, FITC showing green fluorescene. Scale bar: 20 μm. (b) Confocal laser scanning microscopy showing uptake in MCF-7 ($CD206^-/CD13^+$) and MDA-MB-231 ($CD206^+/CD13^-$) breast cancer cells. Scale bar: 20 μm. (c) *In vivo* MRI images in the tumor region, bone and lymph node of mice after intravenous injection of PAA@IONs at 24 h. (d) *In vivo* biodistribution assay of different DiR-labeled liposomes in 4T1 tumor-bearing mice. (e) *Ex vivo* fluorescence imaging of tumors and organs. (f) Quantitative uptake of different formulations in tumor cells (MDA-MB-231) after incubation for 3 h at a Dox concentration of 10 μg/mL. (g) Tissue distribution of PAA@IONs as determined by ICP-MS 24 h post-injection. (h) Mean radiant efficiency of tumors and main organs 24 h after intravenous injection ($n = 3$). $^*P < 0.05$, $^{**}P < 0.01$, $^{***}P < 0.001$, $^{****}P < 0.0001$. Data are the mean ± standard deviation (SD) ($n = 3$). FITC-DL-Lip/DiR-DL-Lip: FITC/DiR fluorescence labeled DL-Lip; FITC-NRDL-Lip: FITC fluorescence-labeled NRDL-Lip; ns: not significant.

that NRDL-Lip could target tumor cells and M2-TAMs. Quantitative analysis using flow cytometry (FCM) confirmed this trend (Fig. 2f).

In addition, we investigated the tumor tissue-targeting efficacy of NRDL-Lip in 4T1 tumor-bearing BALB/c mice. The protocol for animal experiments was approved by the Ethics Committee of Sichuan Huiyu Seacross Medical Technology (No. 2021–234). NRDL-Lip increased fluorescence accumulation in tumors significantly compared with DL-Lip, indicated that NRDL-Lip accumulation was significantly higher than that of unmodified liposomes (LPs), and the duration in tumor tissue was much longer (Figs. 2d, e and h). Furthermore, the healthy BALB/c and B6.FVB-Tg (MMTV-PyVT) mice were administered PAA@IONs *via* tail-vein injection. Magnetic resonance imaging (MRI) indicated that PAA@IONs targeted tumor tissues, lymph nodes and bone significantly 24 h post-injection (Fig. 2c), and that its accumulation was significantly higher in the lymph nodes, liver, lungs, and spleen than in other tissues (Fig. 2g).

ICD has a crucial role in activating the dysfunctional antitumor immune system [20]. An *in vitro* study (Fig. S8 in Supporting information) revealed that NRDL-Lip therapy led to the highest level of tumor-cell apoptosis, calreticulin (CRT) exposure, and release of high-mobility box 1 (HMGB1), and adenosine triphosphate (ATP) in all treatment groups. These data demonstrated that combining Dox with Lap, or modifying cNGR-THP/RP-11, could enhance ICD induction.

To verify that combined treatment with PAA@IONs and NRDL-Lip could reverse the microenvironment of tumor immunity *in vivo*, and could trigger robust and sustained anti-tumor immune responses, we created seven treatment groups (Fig. S9a in Supporting information). For details of the proposed mechanism of action, see Fig. S10 in Supporting information. NRDL-Lip therapy in combination with PAA@IONs was significantly more robust than any form of monotherapy. Intermittent administration (PAA@IONs + NRDL-Lip/IA) may be more suitable for chemo–immunotherapy than sequential administration (PAA@IONs + NRDL-Lip/SA) (Figs. S10b and c). Significant differences were not observed in the mean size of tumors or survival of tumor-bearing mice in the IA group compared with that in the SA group, but the IA group had a better prognosis (Figs. S9b and c in Supporting information). More importantly, some immune-cell indicators from lymph nodes to tumors were significantly better than those from the SA group, such as significantly: more DCs in lymph nodes ($P < 0.0001$); greater numbers of M1-TAMs in tumor tissue ($P < 0.01$): more infiltration of $CD8^+$ T cells ($P < 0.001$); fewer Tregs ($P < 0.001$); higher ratio of $CD8^+$ T cells/Tregs in tumors ($P < 0.0001$) (Figs. S11 and S12 in Supporting information). A too-small sample size of experimental groups may have resulted in no significant differences in tumor size or survival.

M2-TAMs in the TME secrete cytokines such as IL-10 and TGF-β (which can promote the angiogenesis and progression of tumors, and hinder DC maturation) and recruit Tregs into the TME to suppress T-cell activity. M1-like macrophage-derived tumor necrosis factor (TNF)-α can promote the accumulation of reactive oxygen species in latent tumor cells, which can damage various proto-oncogenes and anti-oncogenes [21]. Many types of pro-inflammatory molecules derived from M1-like macrophages have been reported to be involved in cancer-cell killing. Next, levels of various cytokines (TNF-α, TGF-β, interferon-gamma (IFN-γ), IL-10) were measured using enzyme-linked immunosorbent assay (ELISA) kits. Levels of TNF-α and IFN-γ were significantly higher in the PAA@IONs + NRDL-Lip/IA group than in any monotherapy group, whereas levels of TGF-β and IL-10 were significantly lower than in the Dox group (Fig. S12 in Supporting information).

TNBC metastasis results from tumor recurrence, caused primarily by MDR progression, which hinders treatment [22,23]. Drug efflux from cancer cells is a common and important MDR mechanism, inseparable from ATP-binding cassette efflux transporters

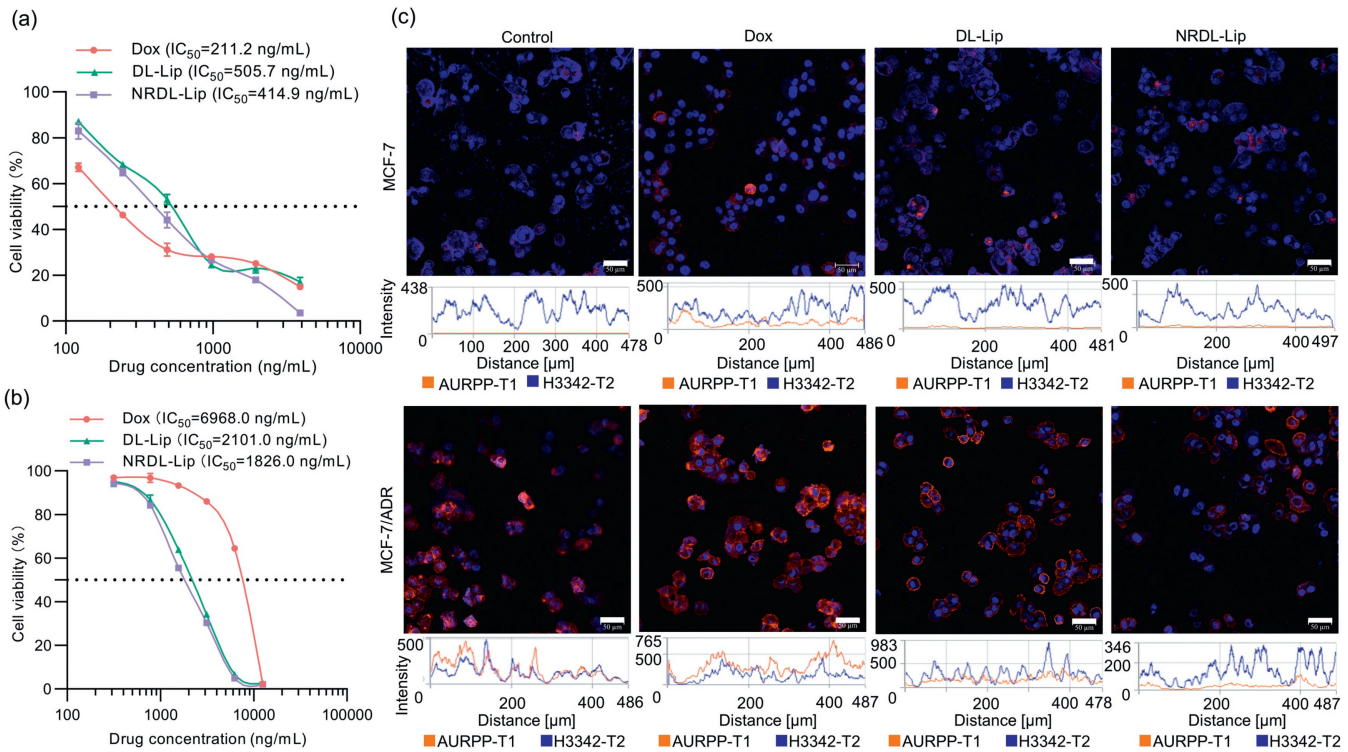

Fig. 3. Reversal of multidrug resistance. (a) *In vitro* cytotoxicity of free Dox, DL-Lip, and NRDL-Lip against MCF-7 cells. (b) Enhanced *in vitro* cytotoxicity of co-delivered liposomes in MCF-7/ADR cells. Data are the mean ± SD ($n = 6$). (c) CLSM showing P-gp expression in MCF-7/ADR and MCF-7 cells incubated with free Dox, DL-Lip, or NRDL-Lip at an equivalent Dox concentration of 500 ng/mL. Scale bar: 50 μm. Blue fluorescence showed the localization of cell nucleus. Red fluorescence showed P-gp expression. Blue: propidium iodide (PI), stained cell nucleus. Red: phycoerythrin (PE)-labeled anti-P glycoprotein.

such as MDR-associated protein 2, P-glycoprotein (P-gp)/ATP-binding cassette transporter B1 (ABCB1), and breast cancer resistance protein/ATP-binding cassette transporter G2 (ABCG2) [24]. MDR decreases the sensitivity of tumors to chemotherapy greatly.

MCF-7/ADR cells were highly resistant to free Dox; the Drug Resistance Index for free Dox in MCF-7/ADR cells was 33.1. However, Lap could be combined with Dox to reverse MDR in MCF-7/ADR cells. MDR reversal in these cells was dose-dependent. Furthermore, the MDR-reversal activity of drugs was enhanced with increased Lap concentration. In addition, modification of cNGR-THP and RP-11 could increase the sensitivity of MCF-7/ADR cells to drugs significantly (Figs. 3a and b). The Drug Resistance Index of drugs (Dox/Lap at a molar ratio of 2:8) in MCF-7/ADR cells was reduced by 20.5-fold, and the Drug Resistance Index decreased to 1.84 (Table S2 in Supporting information). Liposomes were designed based on these results.

Furthermore, P-gp expression in MCF-7/ADR cells after incubation with different types of liposomes was determined by confocal laser scanning microscopy (CLSM) to clarify the proposed mechanism by which NRDL-Lip reversed drug resistance (Fig. S13 in Supporting information). P-gp expression in MCF-7/ADR cells treated with different types of liposomes was in the order NRDL-Lip < DL-Lip < Free Dox (Fig. 3c). These data suggested that modification with cNGR-THP and RP-11 could enhance MDR-reversal activity by reducing P-gp expression in MCF-7/ADR cells.

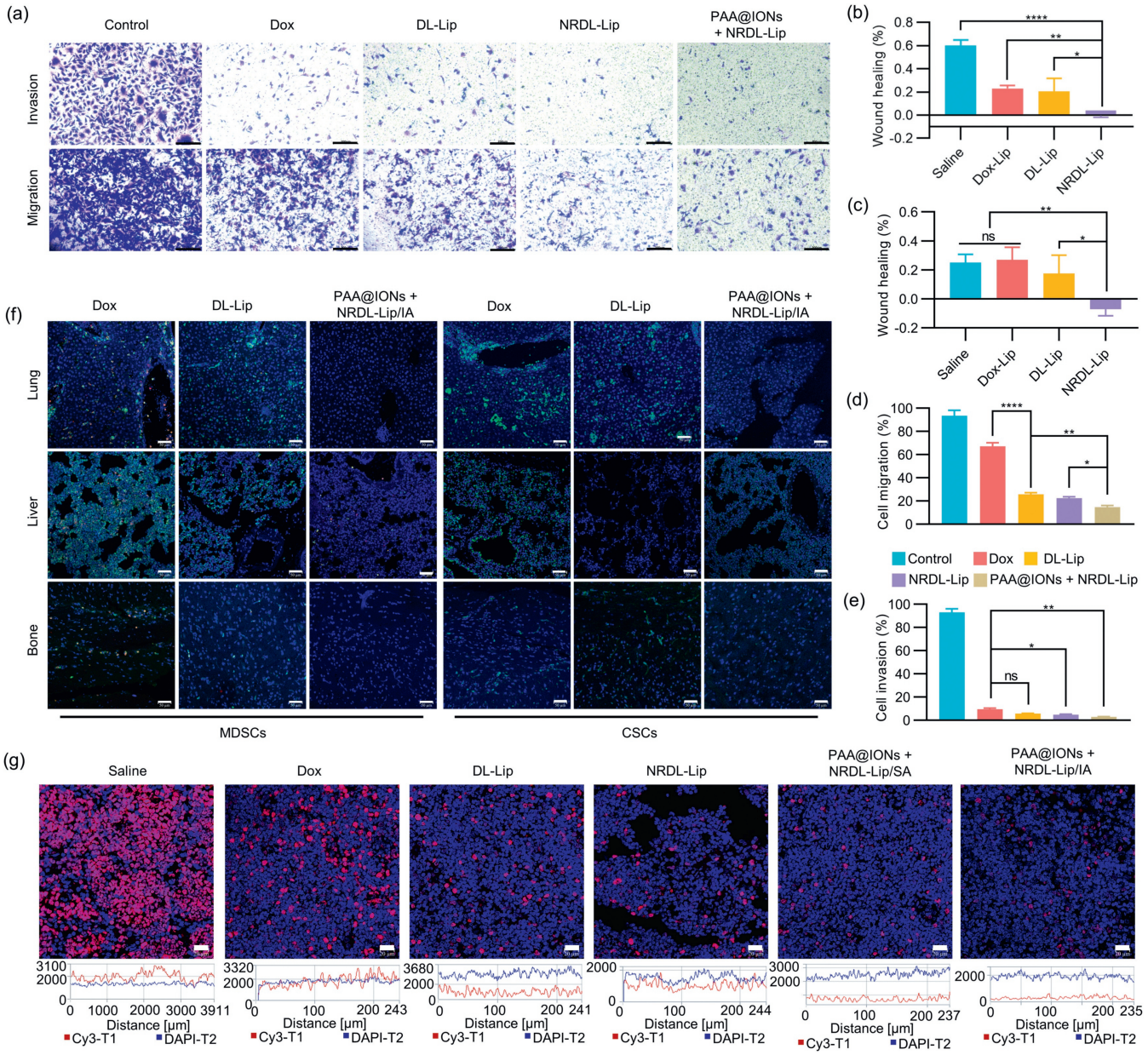

Fig. 4. (a) Images of invading MDA-MB-231 tumor cells in each group. Invading cells at the bottom of the Transwell™ chamber were stained with crystal violet. Scale bar: 200 μm. Quantitative wound-healing inhibition of the migration distance of (b) MCF-7 cells and (c) MDA-MB-231 cells analyzed from the panel. The width of the wound was measured at 0 h and 24 h. Assays to quantify the migration distance of MDA-MB-231 cells (d) MDA-MB-231 cells and (e) invasion assays using Transwell or Matrigel™-coated Transwell. Data are the mean ± SD ($n = 3$); $^{*}P < 0.05$, $^{**}P < 0.01$, $^{****}P < 0.0001$. (f) Infiltration of MDSCs and CSCs in liver, lung and bone tissues. Liver, lung and bone tissues were stained by immunofluorescence analyses. MDSCs were characterized by CD11b (green) and Gr-1 (red), and CSCs were characterized by CD133 (green). Scale bar: 50 μm. (g) Protein expression of Ki-67 protein in lymph nodes. Lymph nodes were stained for immunofluorescence analyses. Ki-67 was characterized by Cy3-conjugated goat anti-rabbit IgG (red). Scale bar: 20 μm.

TNBC is an aggressive metastatic malignancy with a high recurrence rate, and most breast cancer-related deaths are caused by metastasis [25]. The migration and invasion abilities of 4T1 cells were evaluated using wound-healing and Transwell^{TM} assays. The inhibitory effects of PAA@IONs + NRDL-Lip on migration and invasion abilities (Figs. 4a–e and Fig. S14 in Supporting information) were much stronger than those of either agent used alone. Furthermore, the wound-healing rate and number of migratory and invasive cells in the combined treatment group were significantly lower than those in the Dox control group ($P < 0.05$).

Tumor-draining lymph nodes (TDLNs) are the first line of defense against tumor spread [26]. Lymphocyte subsets activated during antitumor responses determine the outcome of host–tumor interactions. Furthermore, Ki-67 is usually overexpressed in lymph nodes and malignant tumors, and is associated with the development, infiltration, metastasis of tumor cells, and a poor prognosis. High protein expression of Ki-67 can predict recurrence and metastasis [27]. Moreover, infiltration of MDSCs is one of the main effects of immunosuppression, angiogenesis, invasion, and metastasis by tumors, and is important in tumor resistance to chemotherapy and immunotherapy [28]. In addition, CSCs are a distinct population responsible for the recurrence and metastasis of tumors due to their self-renewal, differentiation, and tumorigenic abilities, and they give rise to metastatic foci in regional or distant organs or tissues [29,30]. Immunofluoresence analyses of Ki-67, MDSCs, and CSCs were undertaken on the liver, lungs, lymph nodes, and bone marrow tissues of mice in different treatment groups. Infiltration by MDSCs and CSCs in organs and Ki-67 expression in lymph nodes were downregulated significantly by IA of a combination of PAA@ION and NRDL-Lip (Figs. 4f and g).

In summary, the immunosuppressive TME has a major impact on the chemo–immunotherapy of TNBC. We made full use of the anti-tumor effect of M1-TAMs *in vivo* and triggered robust ICD using a new drug delivery system. We loaded anthracycline-based chemotherapeutic agents to evoke robust and efficacious therapeutic strategies to enhance the neoadjuvant therapy of early TNBC or postoperative adjuvant chemotherapy. Due to multiple intravenous administration of PAA@IONs, these nanoparticles are enriched in tumor tissues, lymph nodes, liver, bone, spleen and lungs. Also, macrophages in the TME were polarized to antitumor M1 macrophages, thereby remodeling the immunosuppressive TME. After being modified by the peptide cNGR-THP targeting CD13 on tumor blood vessels and the peptide RP-11 targeting CD206 overexpressed by breast-cancer cells and M2-TAMs, NRDL-Lip enhanced the targeting effect of breast-cancer cells and M2-TAMs significantly, and alleviated cardiotoxicity (Fig. S15 in Supporting information). Activated M1-TAMs and the induced intense ICD had positive effects on promoting DC maturation and antigen presentation, activating cytotoxic T cells, and inducing the secretion of cytokines with anti-tumor effect. IA of a combination of PAA@IONs and NRDL-Lip inhibited the spontaneous metastasis of TNBC cells to lymph nodes, bone, liver, and lungs, and had the potential to reverse chemo-resistance. Our drug delivery system was characterized by dual targeting of tumors and the microenvironment, thereby reversing the suppressive TME and disrupting the intimate interactions between tumor cells and TAMs. Our drug-delivery system could provide a promising nanotechnology for chemo–immunotherapy to combat the MDR and metastasis observed in TNBC.

Declaration of competing interest

The authors declare that they have no known competing financial interests or personal relationships that could have appeared to influence the work reported in this paper.

Acknowledgments

We acknowledge assistance from Xiaofei Xie, Jian Sun and Po Niu for solid-phase peptide synthesis, preparation of PAA@IONs and Lap, respectively. Special thanks go to Dr. Tao Wei and Belinda Liu for their help in manuscript preparation. This work was supported financially by the National Natural Science Foundation of China (No. 81673363).

Supplementary materials

Supplementary material associated with this article can be found, in the online version, at doi:10.1016/j.cclet.2023.108592.

References

[1] L. Vecchi, S.T.S. Mota, M.A.P. Zoia, et al., Cells 11 (2022) 1705.
[2] X. Qiu, Y. Qu, B. Guo, et al., J. Control. Release 341 (2022) 498–510.
[3] L. Biganzoli, N.M.L. Battisti, H. Wildiers, et al., Lancet Oncol. 22 (2021) e327–e340.
[4] D. Zhang, F. Feng, R. Liu, W. Zhu, L. Yao, Chin. Chem. Lett. 30 (2019) 7–14.
[5] I. Fatima, I. El-Ayachi, H.C. Playa, et al., Cancers 11 (2019) 2039.
[6] H. du Bois, T.A. Heim, A.W. Lund, Sci. Immunol. 6 (2021) eabg3551.
[7] Y.Y. Chen, J.Y. Ge, D. Ma, K.D. Yu, Front. Oncol. 10 (2020) 570981.
[8] D.I. Tsilimigras, P. Brodt, P.A. Clavien, et al., Nat. Rev. Dis. Primers 7 (2021) 27.
[9] A.G. Waks, E.P. Winer, JAMA 321 (2019) 288–300.
[10] E. Avitabile, D. Bedognetti, G. Ciofani, A. Bianco, L.G. Delogu, Nanoscale 10 (2018) 11719–11731.
[11] V. Tripathi, J.H. Shin, C.H. Stuelten, Y.E. Zhang, Oncogene 38 (2019) 3185–3200.
[12] F. Emami, S. Pathak, T.T. Nguyen, et al., J. Control. Release 329 (2021) 645–664.
[13] K. Irshad, C. Srivastava, N. Malik, et al., Front. Immunol. 13 (2022) 813888.
[14] Y. Wang, J. Yu, Z. Luo, et al., Adv. Mater. 33 (2021) e2103497.
[15] Y. Jiang, Y. Li, B. Zhu, Cell Death Dis. 6 (2015) e1792.
[16] S. Zhu, N. Yang, J. Wu, Pharmacol. Res. 159 (2020) 104980.
[17] S. Zanganeh, G. Hutter, R. Spitler, et al., Nat. Nanotechnol. 11 (2016) 986–994.
[18] R. Zhang, F. Qi, F. Zhao, et al., Cell Death Dis. 10 (2019) 273.
[19] Z. Chen, J. Wu, L. Wang, H. Zhao, J. He, Med. Oncol. 39 (2022) 83.
[20] L. Fu, X. Ma, Y. Liu, Z. Xu, Z. Sun, Chin. Chem. Lett. 33 (2022) 1718–1728.
[21] J. Wang, D. Li, H. Cang, B. Guo, Cancer Med. 8 (2019) 4709–4721.
[22] J. Chen, X. Yu, X. Liu, et al., Nanoscale 14 (2022) 12984–12998.
[23] L. Liu, F. Zeng, Y. Li, et al., Nanoscale 14 (2022) 4073–4081.
[24] S. Niu, G.R. Williams, J. Wu, et al., Chem. Eng. J. 369 (2019) 134–149.
[25] M. Louca, V. Gkretsi, Cancers 14 (2022) 4528.
[26] M.F. Fransen, M. Schoonderwoerd, P. Knopf, et al., JCI Insight 3 (2018) e124507.
[27] X. Zhu, L. Chen, B. Huang, et al., Sci. Rep. 10 (2020) 225.
[28] Y. Chu, T. Sun, C. Jiang, Chin. Chem. Lett. 33 (2022) 4157–4168.
[29] L. Yang, P. Shi, G. Zhao, J. Xu, et al., Signal Transduct. Target. Ther. 5 (2020) 8.
[30] K. Hu, H. Zhou, Y. Liu, et al., Nanoscale 7 (2015) 8607–8618.